Numerical Method to Simulate GFET Terahertz Wave Detection

Xuehong Ma, Jin He, Chunlai Li, Xiaomeng He, Pan Jun, Guojing Hu, Yuan Ren, and Xiaomeng Wang

SoC Key Laboratory, Peking University Shenzhen Institute and PKU-HKUST Shenzhen-Hong Kong Institution, Shenzhen, China, frankhe@pku.edu.cn

ABSTRACT

A numerical method to simulate THz wave generation and detection of the graphene base field effect transistor (GFET) is developed in this paper. It is derived directly from the hydrodynamic equations and implemented in Matlab coding. Simulations have been discussed in detail and some have also been compared with the existing theories, proving the validity of the developed numerical method.

Keywords: graphene field effect transistor (GFET), THZ performance, numerical method, device physics, modeling and simulation.

1 INTRODUCTION

Terahertz (THz) technologies have been pay much attention in recent years due to is potential application in remote sensing, biomedical, and space communication. Compare with other method, FET based THz generation and detection have displayed a lot of advantages such as frequency tunable, extremely compact and room temperature workable. In 1977, Allen et al demonstrated that the infrared radiation is absorbed by the silicon MOSFET from experiments. Later, Tsui reported weak infrared radiation from the inversion layers in the silicon based FET [1-3].

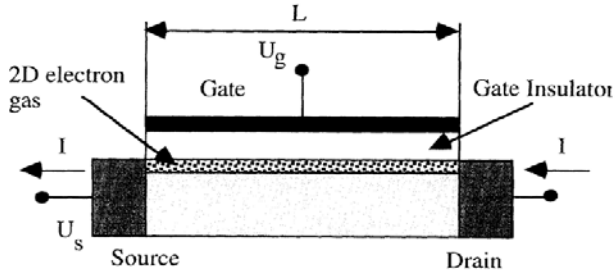

Fig. 1 2DEG in a GFET

In the recent years, grapheme base field effect transistor (GFET) is an ideal candidate for use in RF-FETs and Terahertz device application, because it offers both exceptional electronic properties (room temperature mobility in excess of 10,000 cm2/ V/s and saturation velocity of 1-5 x10^7/ cm), as well as outstanding mechanical performance (strain limits up to 25%) [5-9]. However, there has a little reports on analysis of the THZ performance of GFET so far.

Paralleling the advance of the experimental study, many theories have also developed for silicon THZ Field effect transistor. Dmitriev and Furman utilize the instability properties of 2DEG for THz generation [10], Ryzhii group invent photomixing method for THz detection [11], Dyakonov and Shur propose resonant detection of THz waves [12], and later theory of non-resonant detection was developed by Knap from the resonant detection theory [13], etc. All these theories are based on the hydrodynamic equations derived by Dyakonov and Shur, considering the continuity of charges and the conservation of action of electrons [10]. However, the equations are difficult to yields accurate analytical solutions, hence are theoretically solved by the small signal approximation in all the theories. Therefore, a numerical simulation method is needed to verify the developed theories, and optimize the THZ device structure and design. However, the numerical simulation methods and tools for THZ GFET have not been available in the public domain and commercial EDA so far.

In this paper, a new numerical method to simulate the THZ GFET transistor is developed and tested. In this method the variables and coefficients used are more directly derived from the original hydrodynamic equations, hence, which have clear physical meanings for the device characteristics analysis and structure optimization.

2 THE NUMERICAL METHOD

The hydrodynamic equations are as below [10]:

$$\frac{\partial U}{\partial t}+\frac{\partial (Uv)}{\partial x}=0 \tag{1}$$

$$\frac{\partial v}{\partial t}+v\frac{\partial v}{\partial x}=-\frac{e}{m}\frac{\partial U}{\partial x}-\frac{v}{\tau_m}+\frac{K}{U}\frac{\partial^2 v}{\partial x^2} \tag{2}$$

One can choose whether K=0 or not to decide the method is used for THz detection or generation. The boundary and initial conditions are also different for THz generation and detection [12, 13].

Define $u=U/U_0$, $v=v/s$, $\eta=x/L$, $\tau=ts/L$, $\tau_m'=\tau_m s/L$, $\kappa=K/LsU_0$. Here L is the length of the channel. x=0 denotes the source contact and x=L the drain contact. One can then obtain the dimensionless equations:

$$\frac{\partial u}{\partial \tau}+\frac{\partial (uv)}{\partial \eta}=0 \tag{3}$$

$$\frac{\partial(uv)}{\partial\tau}+\frac{\partial}{\partial\eta}(uv^2+\frac{u^2}{2})+\frac{uv}{\tau_m'}=\kappa\frac{\partial^2 v}{\partial\eta^2} \quad (4)$$

To simulate the THz wave during the dimensionless time interval [0, T], one may define $\Delta\tau$=T/M, $\Delta\eta$=1/N, and F_i^j denotes function F at $\eta_i=i\Delta\eta$, $\tau_j=j\Delta\tau$ to construct the mesh grids.

If vectors below are defined:

$$q_k^n=\begin{bmatrix}u_k^n\\(uv)_k^n\end{bmatrix}\quad F_k^n=\begin{bmatrix}(uv)_k^n\\(uv^2+u^2/2)_k^n\end{bmatrix}$$

$$G_k^n=\begin{bmatrix}0\\(uv/\tau_m')_k^n\end{bmatrix}\quad H_k^n=\begin{bmatrix}0\\\kappa(v_{k+1}^n-2v_k^n+v_{k-1}^n)/(\Delta\eta)^2\end{bmatrix}$$

And L_η is the spatial central-difference operator in the space, Δ_τ the temporal forward-difference operator. One can easily attain the difference version of (3)(4):

$$\Delta_\tau q_k^n+L_\eta F_k^{n+1}+G_k^n=H_k^n \quad (5)$$

Then the Taylor series is applied:

$$F_k^{n+1}\doteq F_k^n+A_k^n(q_k^{n+1}-q_k^n) \quad (6)$$

$$A_k^n=\begin{bmatrix}\partial F_1/\partial q_1 & \partial F/\partial q_2\\ \partial F_2/\partial q_1 & \partial F_2/\partial q_2\end{bmatrix}^n=\begin{bmatrix}0 & 1\\ u-v^2 & 2v\end{bmatrix}_k^n$$

Applying (6) to (5), one can obtain:

$$\begin{aligned}&q_k^{n+1}+TA_{k+1}^n q_{k+1}^{n+1}-TA_{k-1}^n q_{k-1}^{n+1}\\&=q_k^n-TF_{k+1}^n+TF_{k-1}^n+TA_{k+1}^n q_{k+1}^n-TA_{k-1}^n q_{k-1}^n-G_k^n+H_k^n\end{aligned} \quad (7)$$

Here $T=\Delta\tau/2\Delta\eta$. Boundary conditions are then added to the equations. Usually the gate-to-source voltage and the drain current are given to determine the THz-wave in the GFET, which is valid in both THz generation and detection. That is to say, u(0) and uv(1) are given. Because of the existence of $\partial^2V/\partial x^2$, another boundary equation is needed. After examining the side contact of the channel, one can choose $\frac{\partial v}{\partial\eta}(0)=0$ which denotes $v_0^n=v_{-1}^n$. Hence, $\frac{\partial^2 v}{\partial\eta^2}\doteq\frac{v_1^n-v_0^n}{(\Delta\eta)^2}$ at η=0.

At η=0, use equation (5) to add boundary conditions:

$$\frac{(uv)_0^{n+1}-(uv)_0^n}{\Delta\tau}+\frac{(F_2)_1^n-(F_1)_0^n}{\Delta\eta}+(\frac{uv}{\tau_m'})_0^n=\kappa\frac{v_1^n-v_0^n}{(\Delta\eta)^2} \quad (8)$$

Similarly, use equation (6) to add boundary conditions at η=1:

$$\frac{u_M^{n+1}-u_M^n}{\Delta\tau}+\frac{(uv)_M^n-(uv)_{M-1}^n}{\Delta\eta}=0 \quad (9)$$

3 SIMULATION OF GFET THZ GENERATION

In reference [12], an invariant gate-to-source voltage and an invariant drain current is imposed on the FET. Small-signal approximation predicts that the AC voltage and current along the channel has the form exp(-iωt), and the frequency ω has the form $\omega=\omega'+i\omega''$, which indicates that the radiation has the frequency ω' and increment ω''. As confirmed, the increment ω'' decides that only several of the possible frequencies can stably exist in the channel. The frequency ω_n' and increment ω_n'' are given as below (N=1, 2, 3…):

$$\omega_n'=\frac{\pi}{2}(2N-1) \quad (10)$$

$$\omega_n''=\frac{V_0}{s}-\frac{1}{2\tau_m'}-\frac{\kappa\pi^2}{8}(2N-1)^2 \quad (11)$$

If $\omega_k''>0$, all modes ω_n with $n\le k$ will be amplified, and other higher modes will be quickly damped out. Different v_0, κ, τ_m' are chosen to simulate that the THz radiation is damped out, approximately stable, and amplified. u=1 at η=0. $v_0=V_0/s=uv(1)/u(0)$. The results are as Fig. 2.

One can see from the figure that when τ_m' is very small (the second one, ω_1''=-0.97), even the first mode is rapidly damped out and no oscillation happens, or the oscillation will be gradually damped out, as shown in the fourth figure (ω_1''=-0.002). The third figure shows the condition that ω_1=0.012 and ω_2=-0.012, but the oscillation is also damped out. The first figure shows the condition that the first 15 modes are all amplified, but the oscillation is stable and shows only the first mode. We conclude from the simulation and theory that the higher modes are exponentially small than the first one, but tend to damp the oscillation.

One can easily notice that in a 20 time interval, there are approximately five periods of oscillation, indicating a period of T=4. The first dimensionless mode is $\omega=\pi/2$, and that $\omega T=2\pi$ demonstrates that the theory predicts an accurate frequency. When U_0=3V, L=0.05μm, one can calculate that f=3.63THz.

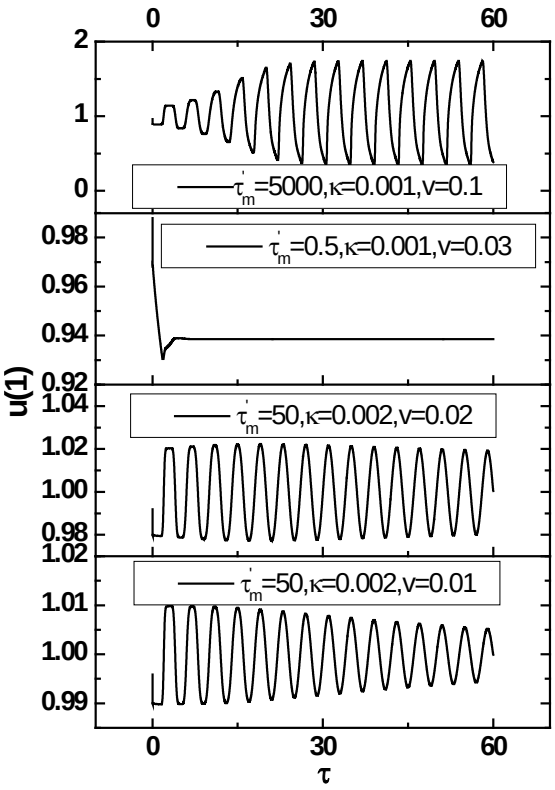

Fig. 2 The simulation of GFET THz generation

4 SIMULATION OF GFET THZ RESONANT DETECTION

Using small signal approximation, Dyakonov and Shur have obtained that the 2DEG in the channel will display resonant response to the incoming signal $U=U_0+U_a\cos\omega t$ from the source contact and $U_a<<U_0$. Hence, the response of U and V has the form:

$$U=\overline{U}+U_1+U_2+\ldots \quad V=\overline{V}+V_1+V_2+\ldots$$

It is more difficult to measure the amplitude than the DC voltage of signals with frequency to the range of THz. The average drain-to-source voltage ΔU has the relationship with U_0 as below [14]:

$$\frac{\Delta U}{U_0}=\frac{1}{4}\left(\frac{U_a}{U_0}\right)^2 f(\omega) \tag{12}$$

$$f(\omega)=\frac{3\sinh^2(L/2s\tau_m)+\sin^2(\omega L/s)}{\sinh^2(L/2s\tau_m)+\cos^2(\omega L/s)} \tag{13}$$

$f(\omega)$ is valid when $\omega\tau_m>>1$. According to the numerical method, we can conclude that the average dimensionless voltage Δu will show peaks at $\Omega=\pi/2$ and its odd harmonics. The simulation made below is under the condition that $u_0=1$, $u_a=0.02$, $\tau_m'=50$ and $\Omega=\pi f/2$, and initial conditions are u=1, v=0:

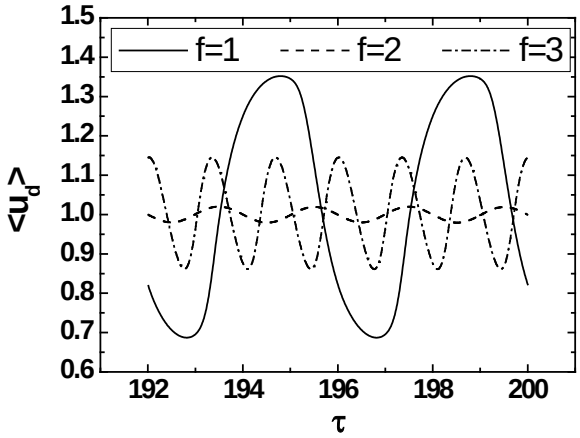

Fig. 3 Stable GFET THz radiation at drain contact

It is clear that at $\Omega=\pi(2N+1)/2$, the amplitude is larger than the even harmonic (Figure 3) which is evident resonant feature, but Fig. 3 does not directly describe Δu and the influence of τ_m' to the peaks is needed to be verified, which are shown in Figure (4).

In Fig. 4, the first one is set at $\tau_m'=50$ and the second one is set at f=1. Yet different result from theoretical anticipation appears: The peaks do happen at f=(2N+1), but the magnitude is much smaller, and neither peak is as sharp as that the theory predicts. Moreover, the second figure does not indicate that $f(\omega)\sim(\tau_m')^2$ either. At last, we notice that the resonant frequency is not accurately at f=1 and f=3, but a little smaller than these frequencies.

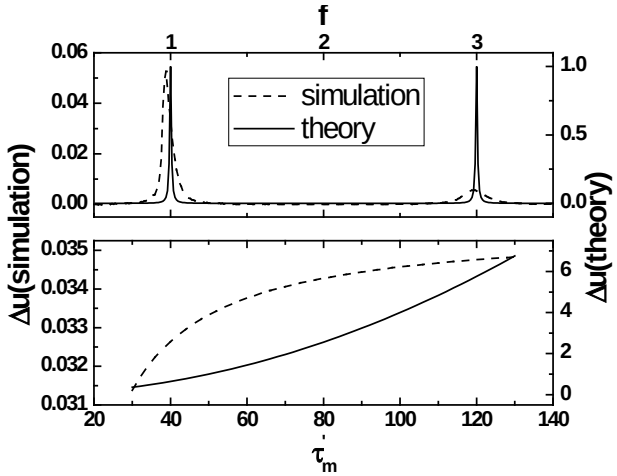

Fig. 4 Influence of f and τ_m' in GFET THz detection

We notice that the theory neglects higher modes of oscillation except the first mode, but Fig. 3 shows that the radiation does not have only a single mode. Therefore the

high modes perhaps damp the peaks because of their phases, and more research is needed to find out what causes the difference between the simulation results and the theory.

5 DISCUSSION AND CONCLUSION

We find from the simulation that the high modes of radiation cannot be neglected. In GFET THz generation, the high modes tend to damp the amplitude, but do not change the frequency. In THz detection, the frequency responsivity exhibits much lower peaks at the high modes, and the fundamental mode is dominant in the detection, which provides possibility of accurate measurement of frequency at THz range, due to that the highest peak is related to only one frequency. The theory predicts a GFET THz wave frequency accurate enough, helping to easily adjust the frequency by voltage. The simulation method is able to provide strong support to the theories mentioned in this issue just by adding different boundary and initial conditions. Also it does not demand the continuity of current, and is therefore possible to be changed for the GFET NQS numerical simulation.

ACKNOWLEDGEMENT

This work is funded by Fundamental Research Project of Shenzhen Sci. & Tech. Fund (JCYJ20170307164247428,), and Guangdong Province SNSFC Fund (2018A030313973).

REFERENCES

[1] S. J. Allen, Jr., D. C. Tsui and R. A Logan, Phys. Rev. Lett., vol. 38, p. 980, 1977
[2] A.P. Dmitriev, A. S. Furman and V. Yu. Kachorovskii, Phys. Rev. B, vol. 54, No. 19, 1996
[3] V. Ryzhii, I. Khmyrova and A. Satou, Journal of Applied Physics, vol. 92, No. 10, 2002
[4] A.K.GeimandK.S.Novoselov, Nature Mater., vol. 6, no. 3, pp. 183–191, 2007.
[5] X.Li,W.Cai,J.An , Science, vol. 324, no. 5932, pp. 1312–1314, 2009.
[6] W. Mehr, J. Dabrowski, IEEE Electron Device Lett., vol. 33, no. 5, pp. 691–693, May 2012.
[7] V. Di Lecce, R. Grassi, IEEE Trans. Electron Devices, vol. 60, no. 12, pp. 4263–4268, 2013.
[8] Q. Zhang, G. Fiori, and G. Iannaccone, Electron Device Letters, IEEE, vol.35, no.9, pp. 966–968, Sept 2014.
[9] S. Venica, F. Driussi, P. Palestri, and L. Selmi, Microelectronic Engineering, vol. 147, no. 0, pp. 192 – 195, 2015.
[10] W. Knap, V. Kachorovskii and Y. Deng, Journal of Applied Physics, vol. 91, No. 11, 2002
[11] M. Dyakonov and M. Shur, Phys. Rev. Lett., vol. 71, No. 15, 1993
[12] A.P Dmitriev, A. S. Furman and V. Yu. Kachorovskii, Phys. Rev. B, vol. 55, No. 16, 1997
[13] V. Ryzhii and A. Satou, Journal of Applied Physics, 103, 014504, 2008
[14] M. Dyakonov and M. Shur, Applied Physics Letters, 87, 111501, 2005
[15] A. Satou, I Khmyrova and V Ryzhii, Semicond. Sci, Technol. 18, 460-469, 2003
[16] A. Satou, V. Ryzhii and A. Chaplik, Journal of Applied Physics, 98, 034502, 2005.